Laboratory Modeling of Aftershock Sequences: Stress Dependences of the Omori and Gutenberg—Richter Parameters

V. B. Smirnov[a, b, c], *****, **A. V. Ponomarev**[a], **S. A. Stanchits**[d], **M. G. Potanina**[b], **A. V. Patonin**[e],
G. Dresen[f], **C. Narteau**[c], **P. Bernard**[c], and **S. M. Stroganova**[a]

[a]*Schmidt Institute of Physics of the Earth, Russian Academy of Sciences, Moscow, 123242 Russia*
[b]*Faculty of Physics, Moscow State University, Moscow, 119991 Russia*
[c]*Institut de Physique du Globe de Paris, Paris, France*
[d]*Skolkovo Institute of Science and Technology, Moscow, 121205 Russia*
[e]*Borok Geophysical Observatory, Schmidt Institute of Physics of the Earth,
Russian Academy of Sciences, Borok, 152742 Russia*
[f]*GFZ German Research Centre for Geosciences, Section III.2: Geomechanics and Rheology,
Potsdam, 14473 Germany*
*****e-mail: vs60@mail.ru*
Received May 22, 2018; revised June 18, 2018; accepted August 15, 2018

Abstract—Laboratory experiments on studying the aftershock regime are carried out on sandstone specimens at different levels of axial loading and uniform compression and at constant pore pressure. The aftershock sequences are modeled by the scenario of stepwise increasing axial loading of a specimen with strain control, which ensures the regular generation of aftershock sequences. The experiments are conducted on intact specimens and on those with preliminarily formed shear macrofractures simulating natural faults. The multichannel recording of the signals of acoustic emission (AE) during the experiments allowed locating the AE sources. Several types of the dependence of the parameters of relaxation of the acoustic activity—parameters p and c of the modified Omori law and the Gutenberg—Richter b-value—on the level of acting stresses are revealed. The b-value decreases with the growth of axial stresses at all levels of uniform compression. In the case of a fracture on the preexisting fault, the Omori relaxation parameter p increases with the growth of axial stresses; parameter c—the time delay before the onset of relaxation—decreases with the growth of axial stresses and increases with the rise of the level of uniform compression. In the case of a fracture of an undamaged specimen, parameter p remains unchanged with the growth of axial stresses, whereas parameter c increases slightly. Parameter variations in the case of a complex stress state with both varying deviatoric (differential stresses) and spherical parts (effective pressure) of the stress tensor take on a unified form when expressed in terms of Coulomb stresses. It is hypothesized that the time delay of the relaxation of the aftershock activity is determined by the kinetics of a fracture in accordance with the kinetic concept of strength in solids. This hypothesis is supported by the exponential dependences of parameter c on stresses and the effective strength of the medium which are revealed in the experiments. Under this hypothesis, based on Zhurkov's formula for the durability of materials, it is possible to unify the dependences of parameter c on the Coulomb stresses at different effective strength values. The obtained parameter estimates for the dependence of c on strength and stresses suggest that the c value is determined by the difference of the strength and the acting stresses, thus indicating how far the stress state of the medium is from critically corresponding to the ultimate strength.

INTRODUCTION

The modified Omori law expresses one of the statistical regularities of seismicity. This law describes the decay of seismic activity (in terms of the number of earthquakes per unit time) $\lambda(t)$ after strong earthquakes as a function of time t elapsed after the mainshock (Utsu et al., 1995):

$$\lambda(t) = \frac{K}{(t + c)^p}. \tag{1}$$

Parameter K is determined by the total number of earthquakes in the aftershock sequence and is sometimes referred to as the productivity of the aftershock sequence. Parameter p is known as the Omori parameter. Parameter c is determined by the characteristic time after the mainshock starting from which the decay of the aftershock activity can be assumed to follow the power law.

The present-day physical interpretation of the parameters contained in (1) and their controlling factors are determined by the notions of the nature and

mechanisms of the excitation and relaxation of after-shocks. A few such mechanisms are currently considered. Among such mechanisms, the cascade models of stress redistribution from the mainshock to the subsequent aftershocks, nonlinear friction on faults, viscoelastic stress relaxation, fluid dynamics in the pore-fracture space, and the gradual evolution of fracturing under the action of stresses (stress-corrosion) are currently believed to be the most probable ones. The question concerning the factors governing the implementation of some mechanism or a combination of mechanisms is still open (a detailed review on the problem is presented in (Kanamori, 2015) and the state-of-the-art approach is briefly described in (Davidsen et al., 2015). However, all the modern models of the aftershock sequences consider the stress-strain state of the medium before the mainshock-shock, the intensity and character of the change of this state as a result of the mainshock, and the parameters of the supposed stress relaxators in the source domain of the main shock as the principal parameters. Correspondingly, the statistical parameters of the modified Omori law (1) are associated with these physical parameters of the models of aftershock processes.

In a number of works (Kisslinger and Jones 1991; Creamer and Kisslinger, 1993; Rabinowitz and Steinberg 1998; Wiemer and Katsumata, 1999; Bohnenstiehl et al., 2002), by analyzing the spatial variations of Omori's p within separate regions, it is hypothesized that p increases with the temperature growth in the source area of the mainshock, which is interpreted as the result of more intense stress relaxation in an elastoviscous medium at high temperatures. Wiemer and Katsumata (1999) also note the dissimilarity of the Omori parameter in shear zones with different peculiarities of tectonic boundaries.

The theoretical calculations based on the rate-and-state model correlated the Omori parameter to the characteristics of the heterogeneity of the distribution of the acting stresses (Helmstetter and Shaw, 2006). The authors of this model note that the parameters of the Omori law are determined by the scatter of the stress values but do not depend on the level of the acting stresses. The empirical evidence demonstrating the dependence of the Omori parameters on the character of the stress field is not presented in the cited paper.

Based on the statistical analysis of the regional data for South California, Ouillon and Sornette (2005) revealed the dependence of Omori's p parameter on the mainshock magnitude. The authors of the cited work interpret this dependence in the context of the epidemic-type cascade aftershock sequence model (ETAS), introducing the assumption that the processes of the activation of seismic rupture exponentially depend on the level of local stresses (which corresponds to Zhurkov's kinetic concept of a fracture). These authors position the introduction of the mechanism which depends on the level of acting stresses as

a fundamental step advancing the ETAS model. We note, however, that validating of the adequacy of this physically substantiated step by the dependence of parameter p on the magnitude of the mainshock is, in our opinion, debatable because the relationship between the earthquake's magnitude and the level of acting stresses, as well as the dependence of the stresses released by the earthquake on its magnitude are not self-evident (the review on this subject is presented in (*Earthquakes...*, 2002).

Some explanations interpret the Omori relaxation of aftershock activity as a consequence of the redistribution of the pore pressure after the mainshock and fluid motion in the aftershock area (Nur and Booker, 1972). This mechanism yields unrealistically low p but is perhaps pertinent in the case of the aftershocks of a reservoir-triggered seismicity, which characteristically has lower p values (Gupta, 2002; Mekkawi et al., 2004; Smirnov et al., 2018).

From the modified Omori law (1), it follows that the decay of the aftershock activity can be approximated by the power law function only a certain time after the main shock rather than immediately after it. The second parameter of the modified Omori law—parameter c—determines the delay of the onset of the power-law decay of activity. As of now, there is no agreed understanding of the nature of this delay and, hence, parameter c.

In the opinion of some authors, the reduced aftershock flow reflected in the constant activity (1) at $t \ll c$ is mainly associated with the loss of information about the relatively weak events as a result of the saturation of a seismic network by the anomalously high flow of seismic signals during the initial interval after the strong main shock (Shcherbakov et al., 2004; Kagan, 2004; Lolli and Gasperini, 2003; Kagan and Houston, 2005; Davidsen et al., 2015).

Other authors believe that besides underreporting weak events, the disparity of the aftershock process at its early stage (immediately after the mainshock) and later stage (corresponding to the power-law decay) is also contributed by physical factors (Narteau et al., 2002; Peng et al., 2006; 2007; Enescu et al., 2007; Nanjo et al., 2007; Narteau et al., 2008; 2009; Holschneider et al., 2012; Hatano et al., 2015; Lippiello et al., 2015; Rodkin and Tikhonov, 2016). Based on the notions derived from modeling hypothesis (Narteau et al., 2002), the authors of (Narteau et al., 2008; 2009) associate parameter c with stress peculiarities in the source area of the mainshock. This hypothesis is supported by the disparity of parameter c in the different types of mainshocks (normal fault, thrust fault, and strike-slip fault ruptures), which was revealed in (Narteau et al., 2009; Lippiello et al., 2015; Hatano et al., 2015), because it is believed that these types of faulting correspond to the different stress-strain states of the lithosphere. The geophysical informativity of parameter c is also supported by the increased effi-

ciency of the prognostic algorithms after introducing the estimates of the stress parameters' variations in the source zones calculated from the c values (Shebalin et al., 2012), as well as by the growth of c with depth (Shebalin and Narteau, 2017).

Despite the substantial progress made in studying the aftershock processes, the conclusions about a specific relationship between the parameters of the modified Omori law and the level and peculiarities of stresses in the source zone of the mainshock, and even the conclusion about the existence of such a relationship are only hypothetical. This ensues from the fact that the tensor of stresses acting in the source zone cannot be directly measured in the in situ conditions, whereas the indirect data about the stress values are insufficiently reliable. In this situation, which is typical for the physics of seismicity, an effective solution for elucidating the peculiarities of the implementation of the probable physical mechanisms lies in the laboratory modeling of the studied processes.

The laboratory modeling of fracture processes with respect to seismicity (Lei and Ma, 2014), including transient seismic regimes (Smirnov and Ponomarev, 2004; Smirnov et al., 2010) has its weaknesses and strengths. The laboratory conditions and modern instrumentation make it possible to conduct experiments with the known and controlled parameters and, in particular, to study the peculiarities of the fracture process in rocks under deliberately varying parameters of the stress-strain state of the medium and its physical properties. Thus, the laboratory modeling allows researchers to verify the suggested physical hypotheses and reveal the fundamental regularities of the studied processes. At the same time, the rocks in the laboratory experiment cannot, in the rigorous sense, adequately model themselves in the natural in situ conditions; therefore, a laboratory experiment cannot fully reproduce the in situ conditions and only remains a qualitative or semiquantitative model (which does not ensure the similarity of all the parameters).

During the recent decades, acoustic emission in mechanically loaded rock specimens was considered as the model of natural seismicity. Numerous studies aimed at establishing the key regularities of acoustic emission and comparing them to seismicity have been conducted since the pioneering works of Vinogradov, Mogi, and Sholz in the 1960s (Vinogradov, 1959; Mogi, 1969; Sholtz, 1968a; 1968b).

It was shown that in the time sequences of AE pulses there are regularities that are characteristic of the sequences of the earthquakes. For instance, a series of AE pulses described by the Omori law were detected in laboratory experiments after the high-amplitude acoustic signals (Lockner and Byerlee, 1977; Hirata, 1987; Rudajev et al., 2000; Lockner, 1993; Stanchits et al., 2006; Smirnov and Ponomarev, 2004; Thompson et al., 2009; Schubnel et al., 2007; Vilhelm et al., 2017). Thus, it was demonstrated that the acoustic aftershocks obey the same statistical laws as the real aftershocks. The experiments have shown that Omori's p ranges within $1-2$ (Hirata 1987; Lockner and Byerlee, 1977; Lei et al., 2004).

A detailed review of the laboratory studies of acoustic emission aimed at understanding the process of earthquake generation is presented in (Lei and Ma, 2014). The authors conclude that the similarity between the parameters of acoustic emission and seismicity offers the possibility to shed light on the evolution of defects and microcracks before and after the failure and nucleation of faults, as well as reveal the factors governing these processes.

It is worth noting that relatively few laboratory experiments were conducted on exploring the variability of the Omori parameters compared to the laboratory studies of the b-value or fractal dimension. Ojala et al. (2004) examined the dependence of parameter p on the temperature of the loaded specimens and has shown that p grows linearly with temperature in the interval of 25 to 80°C from 1.05 to 1.37 and from 0.79 to 1.23 for different types of sandstone at a constant rate of strain loading of 10^{-7} 1/s and under uniform compression at 13.5 MPa. The authors hypothesized that this agrees with the positive correlation between the surface heat flux and the p index because of the higher rate of stress relaxation in the regions with higher temperature which was noted in the field observations (Utsu et al., 1995).

The variability of parameters p, c, and K of formula (1) was investigated in the laboratory experiments on macrofracture formation in the Westerly granite specimens in the conditions of uniaxial loading under uniform compression at 75 MPa. The specimen with a formed macrofracture was loaded by the axial stress which resulted in the emergence of spontaneous stick-slips with a sequence of acoustic aftershocks after each stick-slip event (Goebel et al., 2012). The authors found out that the Omori p and c parameters systematically decrease with each subsequent stick-slip event from 1.53 to 1.10 for p and from 0.32 to 0.15 s for c, albeit, with some deviations from these regularities.

The authors of the cited work associated this tendency with the smoothing of the rupture surface after a series of successive stick-slips as a result of the breakup of asperities and locking inflections on the fault surface. In turn, this leads to the redistribution of the load over the asperities even in one experiment, which may significantly reduce the stress drop, and the residual stresses will systematically decrease after each subsequent stick-slip event.

Another approach to modeling the aftershock sequences employs the stepwise loading of rock specimens under strain control, which ensures the regular generation of sequences of acoustic events with properties similar to the aftershock sequences (Smirnov and Ponomarev, 2004; Smirnov et al., 2010; Vilhelm et al., 2017).

In (Smirnov, Ponomarev, 2004), it is shown that the AE activity after a relatively sharp step in the loading of specimens can be described by the Omori law. We also note that the excitation of acoustic emission by the elastic pulse and its subsequent decay with time is also described by the modified Omori law (Sobolev and Ponomarev, 2013).

The next studies (Smirnov et al., 2010; Vilhelm et al., 2017) have demonstrated that at the relatively low stresses and low rate of stepwise loading (10^{-6}–10^{-5} 1/s), the AE intensity gradually increases, and the peak acoustic activity is reached before the end of the growth stage of the axial loading after which the activity starts decaying even at the stage of the growing load (swarm-like behavior). As the axial stress increases, these maxima migrate to the end of the corresponding loading cycle. This indicates that stepwise loading is, in fact, the initiation of a fracture, whereas the excitation of acoustic emission is a self-developing process, which is mainly controlled by the stress level. In the case of sharp stepwise loading of a specimen (with a strain rate of ~10^{-3} 1/s), the decay of acoustic activity can be described by Omori's power law.

The factors responsible for the disparity between the swarm acoustic activity under a slow increase in loading and the aftershock activity in the case of a rapidly growing loading are currently not quite clear. In a more general view, the described observations can be interpreted as indicating the emergence of induced acoustic emission under stepwise loading with different strain rates (Smirnov et al., 2010).

In this work, we present the results of studying the dependence of the Omori and Gutenberg–Richter parameters on the level of axial stresses and uniform compression in the experiments with water-saturated sandstone specimens conducted at the laboratory of geomechanics and rheology (GFZ, Potsdam). The experiments implemented the scenario of stepwise fracture initiation (Smirnov and Ponomarev, 2004; Smirnov et al., 2010) at varying axial stresses and different values of uniform compression. The specimens were saturated with water before the experiment and then kept at a given constant pore pressure. We consider the results of two experiments (BS02 and BS03) conducted on similar Bentheim sandstone specimens.

Laboratory Instruments

The experiments were conducted on the MTS servo hydraulic machine which provides an axial force of 4600 kN. The axial stress was measured by two sensors: the external MTS sensor installed beyond the pressure cell and the internal GFZ sensor which measured the stresses within the cell. The allowance for friction on the sealing rings of a piston of the press machine allows the stress variations to be corrected as accurately as about ±0.5 MPa. The internal sensor measured the axial stress with an accuracy of ±0.05 MPa and

was calibrated against the readings of the external sensor under the initial load. The axial strain was measured by the sensor of linear displacements connected to the piston of the press machine. In the calculations of the deformation of the specimen, the deformation of the loading system of the press machine which has an effective stiffness of 793 kN/mm was taken into account.

Fourteen sensors of longitudinal oscillations were used for controlling the AE signals and measuring the elastic velocities in the specimen. The specimen was sealed in the neoprene jacket. Through the openings in the jacket, the sensors were glued directly to the specimen's surface and sealed with epoxy resin. Piezoelectric sensors are made of PZT piezoceramic discs with a diameter of 5 mm and a thickness of 2 mm. The resonant frequencies associated with the thickness and diameter of the sensors are ~1 MHz and 400 kHz, respectively. Preamplifiers equipped with high frequency filters with a cutoff frequency of 100 kHz amplified the signals of the piezo transducer to 40 dB. For measuring the P-wave velocities in the different directions within the specimen's volume and for controlling velocity variations during the experiment, some sensors were periodically used as transmitters for ultrasonic sounding with feeding 100-V electric pulses. Velocity measurements were taken every 20–30 s. The waveforms of acoustic pulses and ultrasonic signals were stored in a 16–channel transient recording system (DAXBox PRÖKEL, Germany). The system has a resolution of 16 bits at a sampling rate of 10 MHz per channel (Stanchits et al., 2006; 2009). Ultrasonic and AE signals were recognized automatically after the experiments (Zang et al., 1996).

The location procedure of AE sources includes the automated determination of P-wave arrival times based on the Akaike information criterion (Leonard and Kennett, 1999) and minimizing the travel time residuals based on the simplex algorithm (Nelder and Mead, 1965) with allowance for a time-dependent variation of the velocity of the elastic waves (Stanchits et al., 2006). The accuracy of location is estimated at 2 mm at worst.

Specimen Preparation

Cylindrical specimens with a diameter of 50 mm and a height of 125 mm were cut from a single solid block of Bentheim sandstone. These sandstones are dominated by quartz (~90%) and contain minor amounts of feldspars, iron oxides, and other accessory minerals. The average particle size of quartz grains is 0.2–0.3 mm and the initial porosity is about 19% (Wim Dubelaar, Nijland, 2015).

Prior to testing, the specimens were dried at 50°C in vacuum (~10^{-2} bar) for at least 12 h. Next, after gluing the acoustic sensors on the cylindrical surface of

the specimens the latter were saturated with water and again maintained for at least 12 h before loading.

Catalogues of Acoustic Events

The catalogs of the acoustic events compiled during the experiments contain information about the time and coordinates of the source, as well as the averaged amplitude of the electric signals from acoustic sensors reduced to the selected reference sphere around the event (the absolute calibration of the mechanoelectric transducer was not conducted). By analogy with seismology, amplitude A was converted into the energy class by the formula $K = 2\log_{10} A$. Under the assumption that the spectra of acoustic pulses differ little and that the contact between the sensor and the specimen is constant, A^2 is proportional to seismic energy and K is in this case close in meaning to the notion of the energy class in seismology.

The primary processing of the catalogues followed the procedure that was developed for estimating the homogeneity of seismic catalogue data (Smirnov, 1997; 2009; Smirnov and Gabsatarova, 2000) and previously used for analyzing the data of the laboratory experiments (Smirnov and Ponomarev, 2004; Smirnov et al., 2010).

The catalogues of acoustic events at the working stages of the experiments contained a total of 201 332 events with 110 925 representative (completely reported) ones in the BS02 and a total of 3 337 715 events with 160 138 representative events in BS03.

Loading History

In the in situ conditions, aftershock processes are typically considered in the zones associated with large fault systems such as, e.g., the Californian and North Anatolian shear zones and the subduction zones in the western segment of the Pacific ring. The earthquakes that occur beyond the fault structures are fairly rare and the patterns of their aftershock sequences have not yet been systematized. Therefore, in this work the aftershock sequences were modeled in the specimens with the preliminarily formed macrofractures simulating the natural megafaults.

Figure 1 illustrates the loading history in the BS02 and BS03 tests. In both experiments, a shear macrofracture emerged at the first loading stage as a result of the natural failure of the specimens' material along an oblique plane whose orientation corresponds to the Mohr–Coulomb criterion of a fracture in an undamaged sample.

In the BS02 test, the macrofracture was formed by stepwise raising the axial load under the strain control. In the BS03 test, the specimen at the stage of the macrofracture formation was loaded in the regime under AE feedback control in which the press reduces the strain rate with the growth of acoustic activity (Lock-

ner et al., 1991; 1992; Smirnov et al., 2001). The uniform compression (confining pressure) P_c and pore pressure P_p was constant at this testing stage in both experiments and was $P_c = 40$ and $P_p = 10$ MPa.

In the BS02 test, the macrofracture formation was accompanied by the slip on the fracture surface with the drop of the axial stresses. In the BS03 test, the macrofracture was formed gradually due to loading under AE feedback. In both experiments, the axial stress in the conditions of press-controlled constant strain drops with the formation of macrofractures because of the reduction of the effective elastic properties of the specimen at the macrofracture.

The second stage of the experiments consisted in the modeling of the aftershock sequences in the specimens with the preexisting fault zones. The effect of the stress buildup on the natural faults surrounding the source of the mainshock was simulated in the experiments by stepwise raising the axial load on the specimen by the press, and the relaxation part of the aftershock process was studied.

The steps of load were formed in the strain-controlled press operation mode: the press machine ensured the given rate of rise of the strain step and then held the strain constant up to the beginning of the next step. The rate of rise of the initiating strain step was in all cases identical and equal to 10^{-3} 1/s. The initiating steps were created at different, successively higher levels of axial stresses.

At a certain level of axial stresses, raising the strains by the press ceased causing the increase in the stresses, probably due to the transition of the contact of the formed fracture into the sliding mode when the asperities that existed on the fracture surfaces were broken. In this situation, the stepwise loading was suspended and the level of uniform compression was heightened, which resulted in the formation of new asperities on the contact. Thereafter, stepwise loading was resumed. In each experiment, two such acts of increasing the level of uniform compression were carried out.

Figure 2 shows the dependence of the uniaxial compressive strength of the specimens with preexisting macrofractures (no. *2* in Fig. 2) on the effective pressure, which is equal to the difference of the uniform compression and pore pressure. The strength is presented in terms of the differential stresses—the difference of the axial stresses and the component of uniform compression stress acting along this axis. The strength was estimated as the average differential stress at the strain steps corresponding to the stage of sliding on the macrofracture contact. The events of sliding on the contact indicate that the stresses on the contact reached the strength limit of the asperities. The strength of the intact specimen estimated by the maximal value of the differential stress reached immediately before the emergence of the microfracture is also shown in this figure.
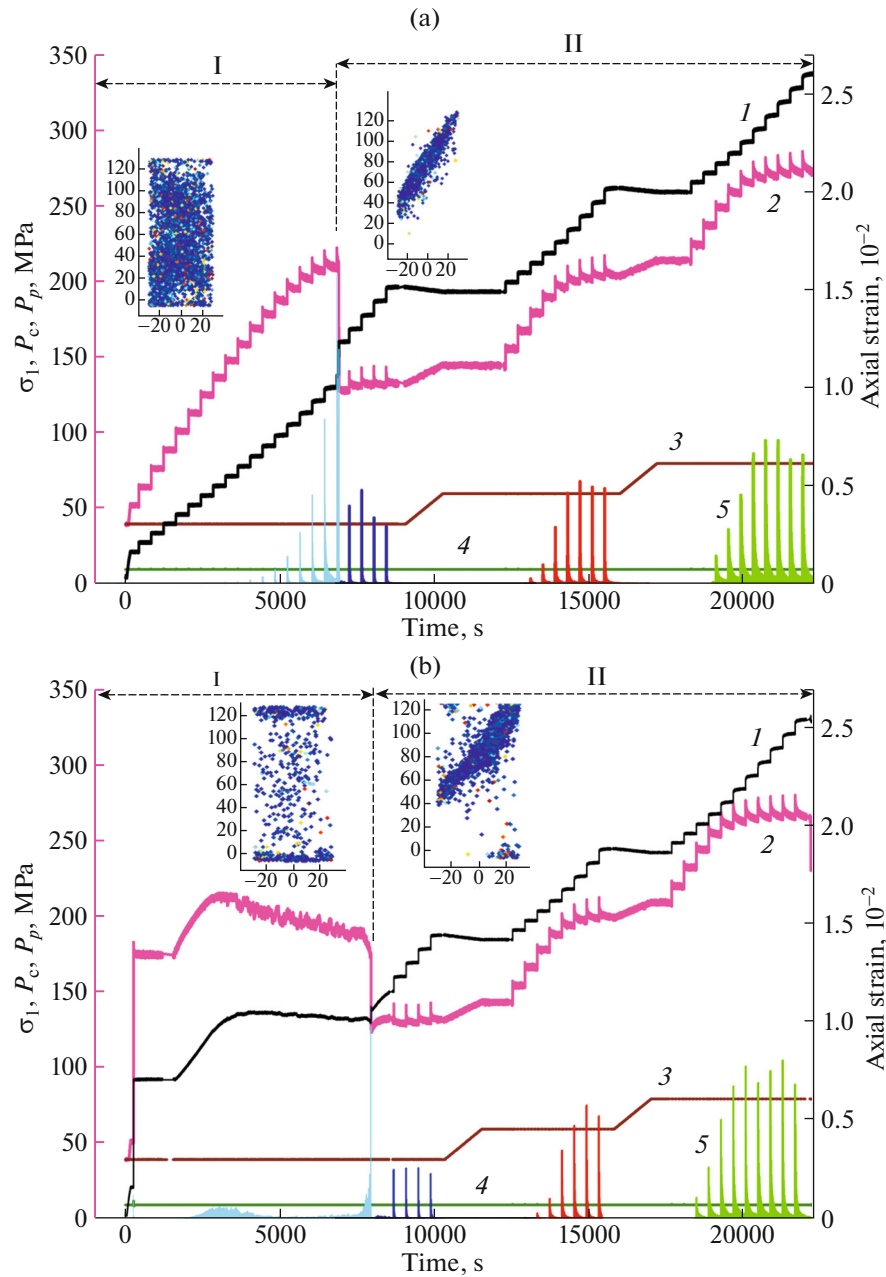
Fig. 1. Loading history in experiments (a) BS02 and (b) BS03: *1*, axial strains; *2*, axial stresses σ_1; *3*, uniform compression pressure P_c; *4*, pore pressure P_p; *5*, acoustic activity (different colors show activity at different values of uniform compression pressure). Insets show examples of distributions of acoustic emission sources within specimens at preparatory (I) and working stages (II).

The linear approximation of the strength's dependence on pressure corresponds to the Mohr−Coulomb criterion of a fracture on the plane oriented at an angle θ to the axis of the principal compression (King, 2009; Jaeger et al., 2007):

$$\tau_c(\theta) = \tau_0, \qquad (2)$$

where τ_0 is the Coulomb strength and $\tau_c(\theta)$ are the Coulomb stresses which depend on the shear $\tau(\theta)$ and normal $\sigma(\theta)$ stresses,

$$\tau_c(\theta) = \tau(\theta) - k\sigma(\theta), \qquad (3)$$

and k is the coefficient of internal friction. Compressive stresses are assumed to be positive according to the practice of the experiment (in contrast to the theoretical mechanics of continua where compressive stresses are negative).

In the scope of the Mohr−Coulomb criterion, the uniaxial compressive strength σ^* linearly depends on the effective pressure of the uniform compression $P = P_c - P_p$:

$$\sigma^* = \sigma_0^* + \alpha P. \tag{4}$$

Using the empirical estimates of the parameters σ_0^* and α, we can determine the material parameters of the specimens k and τ_0:

$$k = \frac{\alpha \sin 2\theta}{2 + \alpha(1 - \cos 2\theta)}, \tag{5}$$

$$\tau_0 = \frac{\sin 2\theta - k(1 - \cos 2\theta)}{2} \sigma_0^*. \tag{6}$$

Angle θ was estimated from the data on the location of the acoustic event, which allows us to determine the tilt of the plane of the formed macrorupture relative to the axis of loading. In the BS02 experiment, this angle is $\theta = 33°$, in the BS03 experiment it is $\theta = 35°$, and the angle determination error is $3°$. The k and τ_0 values estimated by formulas (5) and (6) based on the linear approximations of the data presented in Fig. 2 are $k = 0.66 \pm 0.02$, $\tau_0 = 4.6 \pm 0.5$ MPa in BS02 and $k = 0.63 \pm 0.02$, $\tau_0 = 5.2 \pm 0.6$ MPa in BS03. The errors indicated above are determined by the errors of the regression lines shown in Fig. 2. The comparison of these estimates indicates that the strength characteristics of specimens BS02 and BS03 are similar within the error limits.

Stress Dependences of the Omori and Gutenberg–Richter Parameters

The dependences of the parameters of the modified Omori law (1) and the Gutenberg–Richter b-value were studied as a function of the level of acting stresses at different levels of uniform compression. The parameters were estimated for each series of acoustic events initiated by a given loading step.

Parameters p and c of the Omori law (1) were estimated using the Bayesian approach developed in (Holschneider et al., 2012) (with the free code available[1]), which provides the estimates of the parameters themselves and their statistical errors. In the studies of natural aftershocks, this approach proved its efficiency compared to the other known statistical methods for estimating the parameters of Omori's law (Ommi et al., 2016). For estimating the b-value, we used the maximal likelihood estimation method, taking into account the truncation of the distribution in the area of large magnitudes (Page, 1968; Pickering et al., 1995; Smirnov and Zavyalov, 2012). This technique yields the upper bound and lower bound estimates for the true b-value (Smirnov and Zavyalov, 2012). It works correctly even in the case of the relatively narrow dynamic ranges of the energy of the events, which is important for the conditions of the laboratory experiments.

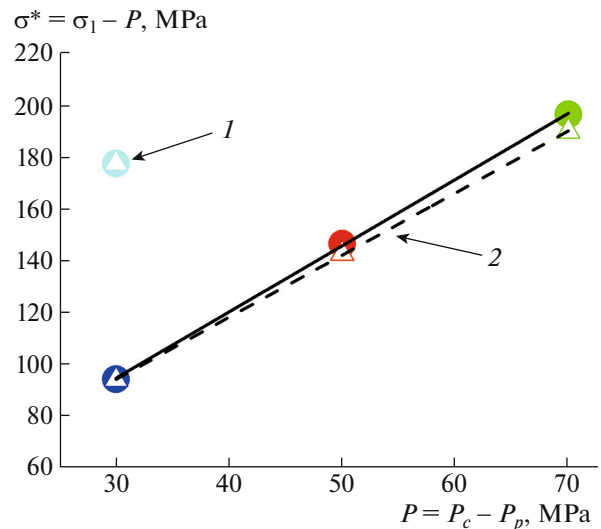[1] http://www.agnld.uni-potsdam.de/~hols/software/patate/.

Fig. 2. Uniaxial compressive strength of specimens σ^* as function of effective pressure of uniform compression P (difference of uniform compression pressure and pore pressure) in experiments BS02 (circles) and BS03 (triangles). Colors correspond to curves *5* in Fig. 1. *1*, intact specimen at preparatory stage; *2*, specimen with formed macrofracture at working stage. For stage *2*, regression lines are shown: solid line for BS02 and dashed line for BS03.

The examples of the decay of acoustic activity $\frac{\Delta n}{\Delta t}$ and its approximation according to the modified Omori law (1) for two stress levels are presented in Fig. 3. The dots in Fig. 3 show the disaggregated $\frac{\Delta n}{\Delta t}$ values at $\Delta n = 1$, corresponding to the intervals between separate acoustic events. The aggregated $\frac{\Delta n}{\Delta t}$ values for $\Delta n = 100$, calculated in the moving windows shifted with a step of 20 events, are also shown. The time resolution of acoustic events during their recording was 0.1 ms and therefore the maximal activity value is limited by 10^4 1/s.

The parameters were estimated in the area confined between the planes parallel to the formed macrofracture and spaced 30 mm from the fracture plane. The selection excluded the acoustic events that were located in the vicinity of the specimen's bases contacting the punch of the press (see the inset in Fig. 1 for the BS03 test). The generation of these edge events is not related to the failure process in the zone of the macrofracture and is associated with the conditions on the contact of the punches with the specimen (Paterson and Wong, 2005).

The results of parameter estimation in both experiments are summarized in Fig. 4. Each point is the result of estimating the parameters from a series of acoustic events initiated by one step of axial loading. The stresses indicated in the horizontal axis are the
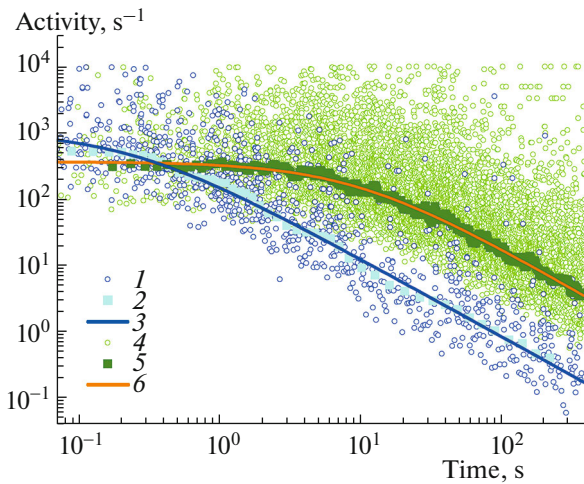
Fig. 3. Examples of decay of acoustic activity for different levels of axial stresses σ_1 and uniform compression pressure P (experiment BS02): *1–3*, σ_1 = 134 MPa, P = 40 MPa; *2–4*, σ_1 = 275 MPa, P = 80 MPa; *1, 4*, disaggregated values; *2, 5*, values aggregated over 100 events within moving window shifted by 20 events; *3, 6*, approximation according to Modified Omori law (1).

levels of differential axial stresses corresponding to the initiating strain steps applied to the specimens.

The first group of the data (shown blue in Fig. 4a) was obtained at the preparatory stage of the BS02 test and corresponds to the regime of failure in the intact specimen (before the formation of the macrofracture).

The second group of the data (shown in dark blue in Fig. 4) corresponds to the regime of sliding on the contact along the macrofracture at the same effective pressure of uniform compression $P = P_c - P_p$, at which the macrofracture was formed at the preparatory stage of each test, $P = 30$ MPa. In this regime, because of sliding, the strain steps do not initiate an increase in the acting stresses.

The third and fourth groups of the data correspond to the regimes of the buildup of the acting stresses as a result of steplike strains at the stages with the P values increased to 50 and 70 MPa (red and green, respectively).

At the initial levels of differential stresses, at each value of the effective pressure of uniform compression, identical strain steps initiate relatively few acoustic events and, respectively, the errors of the statistical estimates of the parameters are large. As the acting stresses increase and approach the strength limit, acoustic activity intensifies and the statistics become sufficient for more reliable parameter estimates.

In Fig. 4a it can be seen that the Omori and Gutenberg−Richter parameters vary in a regular manner depending on the level of axial stresses and uniform compression. Here, the Omori parameters estimated in the different experiments during the working stage (in the presence of the macrofracture) at the approxi-

mately equal stress levels coincide with each other within their statistical errors.

At the preparatory stage, in the intact specimen, the Omori parameter p varies insignificantly, whereas parameter c increases with the growth of the acting stresses (blue curves in Fig. 4a).

At the working stage, in the presence of a macrofracture, parameter p grows with an increase of the acting stresses: within the limits of each level of uniform compression pressure, this trend is apparent in the entire range of stresses, and in the stress interval $\sigma > 0.9\sigma^*$, the increase in p overruns the limits of the error interval; i.e., it is statistically significant. The dependence on the uniform compression pressure consists of the fact that with the growth of pressure the same values of parameter p are reached at the higher levels of axial stresses.

The second parameter of the modified Omori law, parameter c, decreases with the growth of the acting stresses at the working stage. This trend is observed in the entire range of stresses; the reduction is by about one order of magnitude within each level of the uniform compression pressure. In the stress interval $\sigma > 0.9\sigma^*$, the reduction is statistically significant. With the transition from the lower level of uniform compression pressure to the higher pressure level, the level of the c values increases approximately by the order of magnitude (in Fig. 4, the curves of the variations in parameter c obtained at different values of uniform compression pressure are shifted relative to each other along the vertical axis).

Remarkably, in our studies we did not detect the effect of saturation of the acoustic signal's recording system even at the highest levels of the flow of acoustic events. However, if we still assume the presence of this effect, the artifact dependence of parameter c on stress would have been inverse to the actually established one: instead of decreasing, c would have increased with the growth of the stress. The recording system's saturation interval becomes longer the higher the acoustic activity; however, the activity increases with an increase of the stresses. Hence, the length of the saturation interval of the system increases with the growth of the stress. In contrast to this, we detected a decrease of c with an increase of the stress.

The empirical dependences of parameter c on the axial stresses for two levels of the pressure of the uniform compression are shown, together with their exponential approximations (straight lines on the semilogarithmic scale in Fig. 4a):

$$c(\sigma) = c_o e^{-\beta\sigma}. \qquad (7)$$

The respective parameters of the regressions are summarized in Table 1.

The asterisk in Fig. 4 for experiment BS02 shows the estimates of the Omori parameters for the sequence of acoustic events that emerged after the nat-
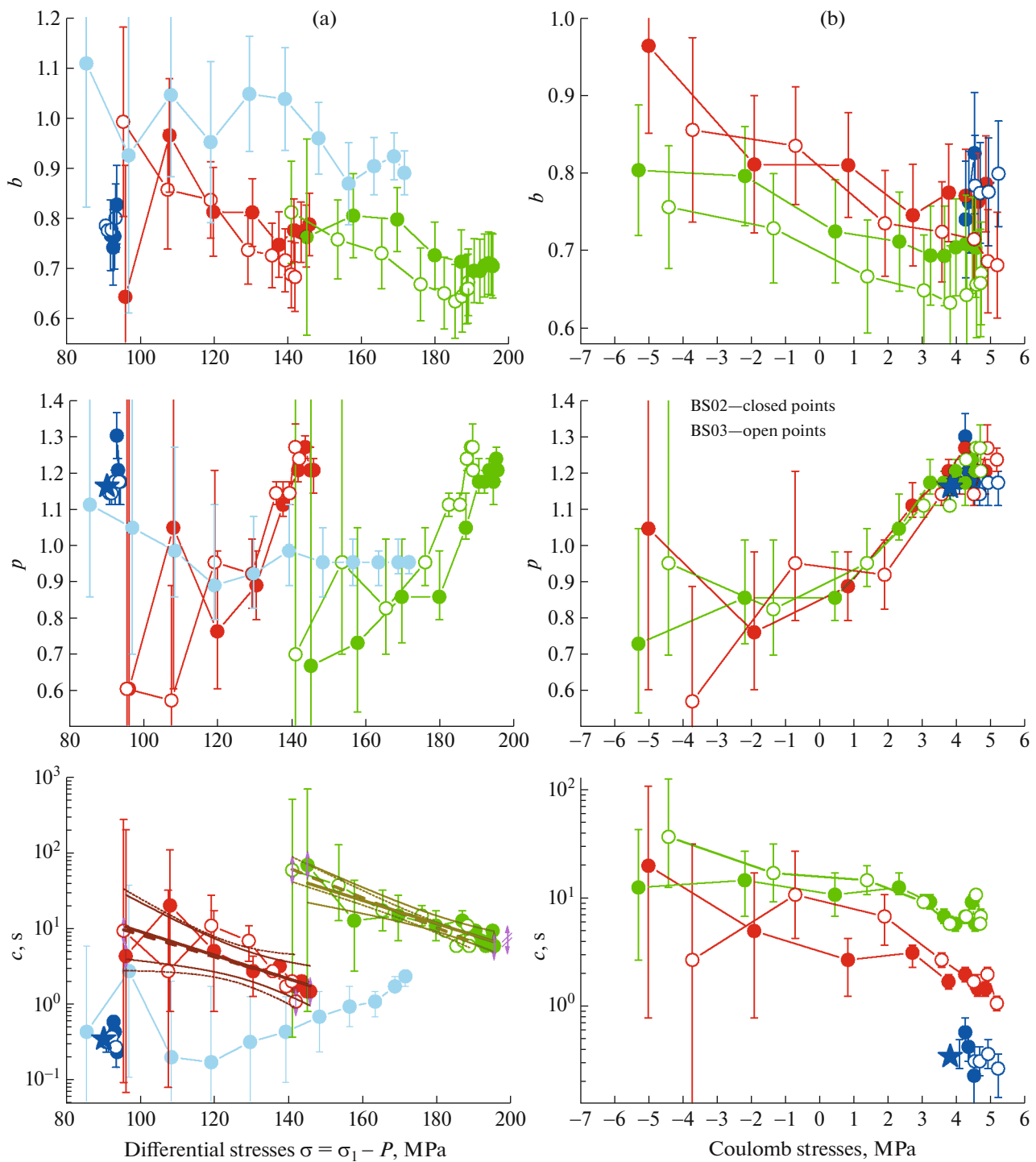
Fig. 4. Dependences of parameters of Omori and Gutenberg–Richter laws on (a) differential and (b) Coulomb stresses according to data of experiments BS02 (filled circles) and BS03 (open circles); intervals of 95% confidence are shown at points. Colors correspond to curves *5* in Fig. 1. Asterisk marks values for sequence of acoustic events that emerged after natural formation of macrofracture at preparatory stage of BS02 experiment. Figure 4a for parameter *c* shows regression lines and their confidence intervals: solid lines for BS02 and dashed lines for BS03.

ural formation of a macrofracture at the preparatory stage of the experiment. It can be seen that these values are close to those estimated from the sequences

that were initiated by the strain jumps created by the press machine with the same levels of axial stresses and uniform compression pressure.

Table 1. Parameters of exponential approximation of $c(\sigma) = c_o e^{-\beta\sigma}$

Experiment	$P = P_c - P_p$, MPa	$\log c_o$ (c)	β, 1/MPa
BS02	50	2.5 ± 0.6	0.037 ± 0.012
BS03	50	2.4 ± 0.8	0.035 ± 0.014
BS02	70	3.8 ± 0.5	0.035 ± 0.007
BS03	70	4.6 ± 0.3	0.046 ± 0.007

Parameter b diminishes with an increase of the acting stresses. In this case, the scatter of the values obtained in the two experiments is larger than for the parameters of the Omori law.

Experiments were also conducted with specimens in a complex stress state with both the deviatoric (differential stresses) and spherical (effective pressure) parts of the stress tensor varying. The stress dependences of the Omori and Gutenberg–Richter parameters in this case also turned out to be complicated and behaved differently under the increase of axial stresses and under the increase of uniform compression. The situation however becomes clearer when we pass to the Coulomb stresses.

Figure 4b shows the obtained results of parameter estimation as the functions of the Coulomb stresses acting on the sites of macrofractures. The Coulomb stresses were calculated for the working stage of the experiments by formula (3) based on the analysis of the data presented in Fig. 2.

It can be seen in Fig. 4b that in terms of the Coulomb stresses, the increase of parameter p is the same at the different levels of the pressure of the uniform

Fig. 5. Dependence of limiting values of Omori parameter c^* on compressive strength. Colors of points correspond to curves 5 in Fig. 1, experiments BS02 (circles) and BS03 (triangles). Straight line shows exponential approximation (9).

compression. The scatter of the points is random and commensurate with the statistical errors of the estimates of parameter p.

At the end of each loading cycle with a given level of uniform compression pressure, upon transition to the regime of sliding on the macrofracture contact (as the Coulomb stresses reach ~3.8 MPa), the growth of parameter p ceases. This should perhaps be considered as evidence of the change in the parameters or in the mechanism of relaxation upon the transition of the failure to the regime of sliding on the macrofracture contact surfaces. It is unclear whether a similar distinction takes place in the in situ conditions; however, this distinction could be sought in the comparison of the parameters of aftershock sequences in the large, well developed fault zones and in the regions of areal continental seismicity.

The changes of parameter c in terms of the Coulomb stresses branch into three groups, corresponding to the different levels of uniform compression. The reduction of c with the growth of the Coulomb stresses has a similar character at the different pressure levels; at the same time, the curves are shifted relative to each other along the vertical axis.

DISCUSSION

In the Introduction it was noted that a number of models of aftershock processes predict the dependence of the Omori parameters on the stresses acting in the medium. For example, according to the model (Narteau et al., 2009), parameter c should be expected to decrease with the growth of the stress, and the results of our experiment support the conclusion of this model. Moreover, the experiments revealed the exponential pattern of the stress dependence of parameter c in the studied specimens (formula (7)).

In (Ouillon and Sornette, 2005), for interpreting the parameters of the Omori law, the authors considered the model of the aftershock process in combination with the notions of Zhurkov's kinetic concept of fracture. In accordance with Zhurkov's formula (Zhurkov, 1965; 1968), the probability of a macrofracture which is determined by thermal activation on the microlevel exponentially depends on the stress level σ in the medium:

$$F = F_0 e^{\frac{\gamma\sigma}{KT}}, \tag{8}$$

where T is temperature, K is Boltzmann's constant, and γ is Zhurkov's parameter depending on the structure of the inhomogeneities of the material.

Parameter F_0 in formula (8) is associated with the strength properties of the medium and is determined by both the material constants (interionic bond dissociation energy) and pressure (Regel et al., 1974). In our experiments, the effective strength of the formed fault zone (macrofracture) is determined by the strength
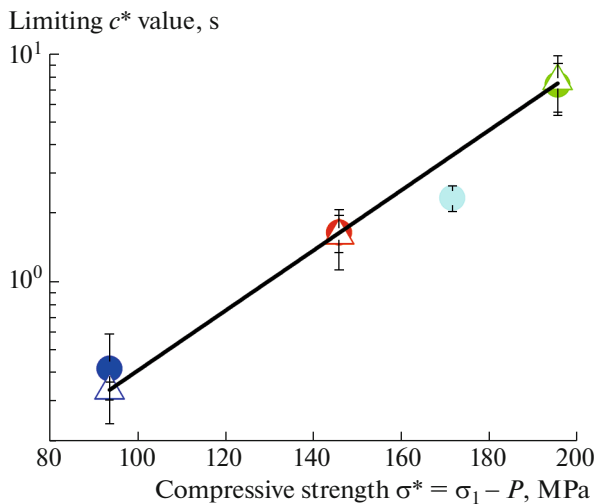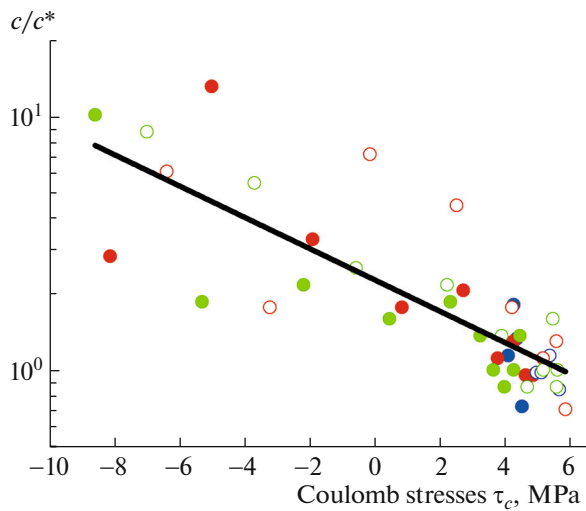
Fig. 6. Omori parameter c normalized to c^* corresponding to ultimate strength. Colors of points correspond to curves 5 in Fig. 1, experiments BS02 (circles) and BS03 (triangles). Regression line according to (10) is shown.

properties of the asperities and the value of the uniform compression pressure. It was established that the level of the values of parameter c increases with the increase of the effective pressure P. In Table 1, we presented parameters c_0 and β of the approximation $c(\sigma, P) = c_o(P) e^{-\beta\sigma}$, which corresponds to formula (8) in the part concerning the dependence of stress σ. From Table 1 it can be seen that c_0 increases with the growth of pressure, whereas parameter β is, within the statistical errors, pressure independent. In the context of the model (Narteau et al., 2009), this can be interpreted as the increase of parameter c with the growth of the strength of the medium. According to this model, parameter c is determined by the overstress values; it decreases with the stress growth and increases with the increase in strength. The data of the experiments allow us to specify the form of the strength dependence of parameter c for the studied specimens.

Figure 5 shows the limiting c^* values corresponding to the maximal Coulomb stresses when the axial stresses reach the level of effective strength on the macrofracture as a function of this effective strength σ^*. (The average values of c over two tests in the range of the Coulomb stresses from 3.8 to 4.3 MPa at three levels of uniform compression pressure are taken.) It can be seen that the dependence of c^* on σ^* is close to exponential. Its approximation averaged over the two tests has the following form:

$$c^* = (0.03 \pm 0.02) e^{(0.03 \pm 0.001)\sigma^*}. \tag{9}$$

In this graph, we also show the limiting c^* value estimated at the preparatory stage for the intact specimen at stresses equal to the strength limit. It can be

seen that this point is also close to the strength dependence of parameter c^* obtained for the fault zone.

The dependences of the Omori parameter c on the Coulomb stresses and strength presented in Figs. 4 and 5 can be integrated into a single dependence:

$$\ln \frac{c}{c^*} = l_1 \tau_c + l_0, \tag{10}$$

$$\ln c^* = m_1 \sigma^* + m_0. \tag{11}$$

Figure 6 with the axes corresponding to formula (10) shows the points that were constructed with allowance for (11) with $m_1 = 0.03$ MPa^{-1} and $m_0 = -3.93$ according to (9). It is apparent that the points corresponding to the different strength values for both experiments hit a single dependence. Regression gives the following estimates for the coefficients of (10): $l_1 = -0.14 \pm 0.02$ MPa^{-1} and $l_0 = 0.83 \pm 0.07$.

The closeness of the power exponents in the dependences of parameter c and its limiting value c^* on the stress σ and strength (stress limit) σ^*, respectively, (formulas (7) and (9)) is a remarkable fact. Coefficient β in (7) has a characteristic value of about -0.037 1/MPa and the respective coefficient in (9) is 0.03 1/MPa. If we assume that the absolute values of these coefficients coincide, then the dependence of the Omori parameter c on the stresses and strength takes on the following form $c \sim e^{\beta(\sigma^* - \sigma)}$, indicating that the value of parameter c is determined by the difference between the strength and the acting stresses, i.e., by how far the stresses are from the ultimate strength.

CONCLUSIONS

The experiments on modeling the aftershock regimes at the different levels of axial stresses and uniform compression pressure and at constant pore pressure have been conducted on two identical sandstone specimens. The analysis of the obtained results revealed a number of dependences of the parameters of the acoustic regime on the stress and character of the fracture and also suggested some hypotheses of their nature.

The model aftershock relaxation parameters—the Gutenberg–Richter b-value and the Omori p and c—depend on the parameters of the stress state of the samples, namely, on the level of axial stresses and the effective pressure of uniform compression. The b-value decreases with the growth of axial stresses at all levels of uniform compression. In the case of a failure on the preliminarily formed fault, the relaxation parameter p decreases with the increase of the axial stresses; the parameter of the time offset before the onset of relaxation c exponentially decays with the increase of axial stresses and exponentially grows with the increase of the pressure of uniform compression. In the case of a fracture of the intact specimen, parameter p does not

vary with the increase of axial stresses and parameter c insignificantly increases.

The changes in these parameters of the acoustic regime in the case of a complex stress state when, in addition to the variations in the deviatoric part of the stress tensor (differential stresses), its spherical part (effective pressure) also varies, assume a unified form if we pass to the Coulomb stresses. In terms of the Coulomb stresses, the increase in p turns out to be identical at different levels of uniform compression. The decay of c with the growth of the Coulomb stresses at different pressures follows the similar exponential pattern; however, the curves of the dependences corresponding to the different pressure levels are shifted relative to each other. The level of parameter c and its limiting (minimal) value increase with the increase of pressure, which can be interpreted as the dependence of c on the effective strength of the fault zone (which is determined in the conducted experiments by the pressure of uniform compression).

The dependence of the c values on the axial stress and pressure can be explained if we assume that the delay before the onset of the power-law decay of the aftershock activity, which is characterized by this parameter, has a kinetic nature. This hypothesis is supported by the exponential dependences of parameter c on the stresses and on the effective strength that were revealed in the experiments. In the context of this hypothesis, based on Zhurkov's formula for the durability of materials, it is possible to unify the dependences of parameter c on the Coulomb stresses at the different effective strengths. The obtained estimates for the stress and strength dependence of parameter c suggest that the c value is determined by the difference of the strength and the acting stresses, thus indicating how far the stress state of the medium is from the critical state corresponding to the ultimate strength.

The further support or arguments for confirming or rejecting the considered hypotheses about the kinetic nature of the delay of aftershock activity can be obtained based on the laboratory and field studies of the dependence of parameter c on temperature and pressure, as well as on the strength of the medium.

In the in situ conditions, the temperature and pressure (as well as the related effective strength) vary with the depth, which determines the promising possibilities of studying the regularities in the variations of the Omori parameters as a function of the depth of the aftershock sequences. Since the strength, according to the Mohr–Coulomb criterion, increases with pressure, our laboratory results suggest that the values of parameter c should be expected to increase with depth. However, according to the kinetic concept of strength, the growth in temperature causes the durability of the material to decrease, which in the context of fracture mechanics should be interpreted as a reduction of strength with temperature. Since both pressure and temperature generally increase with depth, the changes in the strength and, together with it, the changes in the parameter c can be nonmonotonic, depending on the predominant trend (the strength growth with pressure against strength reduction with temperature) in a given depth interval. The recent results on the behavior of parameter c with depth in California support these suggestions (Shebalin and Narteau, 2017).

If the delay before the onset of the power-law aftershock decay is associated with the kinetics of the fracture and if the exponential dependence of parameter c revealed in our experiments corresponds to formula (8), we should also expect the dependence of c on temperature included in (8) symmetrically with stresses σ. In particular, anomalous values of parameter c should be expected in the regions with a high temperature.

ACKNOWLEDGMENTS

REFERENCES

Bohnenstiehl, D.R., Tolstoy, M., Dziak, R.P., Fox, C.G., and Smith, D.K., Aftershock sequences in the mid-ocean ridge environment: an analysis using hydroacoustic data, *Tectonophysics*, 2002, vol. 354, pp. 49–70.

Creamer, F.H. and Kissslinger, C., The relationship between temperature and the decay parameter for aftershock sequences near Japan, *EOS Trans. Am. Geophys. Union*, 1993, vol. 74, F417.

Davidsen, J., Gu, C., and Baiesi, M., Generalized Omori-Utsu law for aftershock sequences in southern California. *Geophys. J. Int.*, 2015, vol. 201, no. 2, pp. 965–978.

Earthquakes: Radiated Energy and the Physics of Faulting, Abercombie, R., McGarr, Art., Di Toro, G., and Kanamori, H., Eds., AGU Geophysical monograph 170, Washington: AGU, 2000.

Enescu, B., Mori, J., and Miyazawa, M., Quantifying early aftershock activity of the 2004 mid-Niigata Prefecture earthquake (Mw 6.6), *J. Geophys. Res.*, 2007, vol. 112, B04310. doi 10.1029/2006JB004629

Goebel, T.H.W., Becker, T.W., Schorlemmer, D., Stanchits, S., Sammis, C., Rybacki, E., and Dresen, G., Identifying fault heterogeneity through mapping spatial anomalies in acoustic emission statistics, *J. Geophys. Res.*, 2012, vol. 117. B03310. doi 10.1029/2011JB008763

Gupta, H.K., A review of recent studies of triggered earthquakes by artificial water reservoirs with special emphasis on earthquakes in Koyna, India, *Earth Sci. Rev.*, 2002, vol. 58, pp. 279–310.

Hatano, T., Narteau, C., and Shebalin, P., Common dependence on stress for the statistics of granular avalanches and earthquakes, *Sci. Rep.*, 2015, no. 5, p. 12280.

Helmstetter, A. and Shaw, B.E., Relation between stress heterogeneity and aftershock rate in the rate-and-state model, *J. Geophys. Res. Solid Earth*, 2006, vol. 111, no. B7.

Hirata, T., Omori's power law aftershock sequences of microfracturing in rock fracture experiment, *J. Geophys. Res.*, 1987, vol. 92, pp. 6215–6221.

Holschneider, M., Narteau, C., Shebalin, P., Peng, Z., and Schorlemmer, D., Bayesian analysis of the modified Omori law, *J. Geophys. Res.*, 2012, vol. 117, B06317. doi 10.1029/2011JB009054

Jaeger, J.C., Cook, N.G.W., and Zimmerman, R., *Fundamentals of Rock Mechanics*, Malden: Wiley-Blackwell, 2007.

Kagan, Y.Y., Short-term properties of earthquake catalogs and models of earthquake source, *Bull. Seismol. Soc. Am*, 2004, vol. 94, no. 4, pp. 1207–1228.

Kagan, Y.Y. and Houston, H., Relation between mainshock rupture process and Omori's law for aftershock moment release rate, *Geophys J. Int*, 2005, vol. 163, no. 3, pp. 1039–1048.

Kanamori, H., *Earthquake Seismology*, Treatise on geophysics, vol. 4, San Diego: Elsevier, 2015.

King, G.C.P., Fault interaction, earthquake stress changes, and the evolution of seismicity, in *Earthquake Seismology*, vol. 4 of *Treatise on Geophysics*, Kanamori, H., Ed., 4th ed., Oxford: Elsevier, 2009, pp. 225–257.

Kisslinger, C. and Jones, L.M., Properties of aftershock sequences in southern California, *J. Geophys. Res.*, 1991, vol. 96, no. 11, pp. 947–958.

Lei, X. and Ma, Sh., Laboratory acoustic emission study for earthquake generation process, *Earthquake Sci.*, 2014, vol. 27, no. 6, pp. 627–646. doi 10.1007/s11589-014-0103-y

Lei, X., Masuda, K., Nishizawa, O., Jouniaux, L., Liu, L., Ma, W., and Satoh, T., Detailed analysis of acoustic emission activity during catastrophic fracture of faults in rock, *J. Struct. Geol*, 2004, vol. 26, pp. 247–258.

Leonard, M. and Kennett, B.L.N., Multi-component autoregressive techniques for the analysis of seismograms, *Phys. Earth Planet. Inter.*, 1999, vol. 113, nos. 1–4, pp. 247–263.

Lippiello, E., Giacco, F., Marzocchi, W., Godano, C., and de Arcangelis, L., Mechanical origin of aftershocks, *Sci. Rep.*, 2015, vol. 5, p. 15560. doi 10.1038/srep15560

Lockner, D.A., The role of acoustic emission in the study of rock fracture, *Int. J. Rock Mech. Min. Sci. Geomech. Abstr*, 1993, vol. 30, pp. 883–899.

Lockner, D.A. and Byerlee, J.D., Acoustic emission and fault formation in rocks, *Proc. 1st Conf. on Acoustic Emission in Microseismic Activity in Geological Structures and Materials*, Hardy, H.R. and Leighton, F.W., Eds., Clausthal-Zellerfeld: Trans Tech Publications, 1977, pp. 99–107.

Lockner, D.A., Byerlee, J.D., Kuksenko, V., Ponomarev, A., and Sidorin, A., Quasi-static fault growth and shear fracture, *Nature*, 1991, vol. 350, no. 6313, pp. 39–42.

Lockner, D.A., et al., Observations of quasistatic fault growth from acoustic emissions, in *Fault Mechanics and Transport Properties of Rocks*, Evans, B. and Wong, T.-F., Eds., London: Academic, 1992, pp. 3–31.

Lolli, B. and Gasperini, P., Aftershocks hazard in Italy. Part I: estimation of time-magnitude distribution model parameters and computation of probabilities of occurrence, *J. Seismol*, 2003, vol. 7, no. 2, pp. 235–257.

Mekkawi, M., Grasso, J.-R., and Schnegg, P.A., A long-lasting relaxation of seismicity at Aswan reservoir, Egypt, 1982–2001, *Bull. Seismol. Soc. Am.*, 2004, vol. 94, pp. 479–492.

Mogi, K., Study of elastic shocks caused by the fracture of heterogeneous materials and its relation to earthquake phenomena, *Bull Earthquake Res. Inst.*, 1962, vol. 40, pp. 125–173.

Nanjo, K., Enescu, B., Shcherbakov, R., Turcotte, D., Iwata, T., and Ogata, Y., Decay of aftershock activity for Japanese earthquakes, *J. Geophys. Res. Solid Earth*, 2007, vol. 112, no. B8.

Narteau, C., Shebalin, P., and Holschneider, M., Temporal limits of the power law aftershock decay rate, *J. Geophys. Res.*, 2002, vol. 107, p. B2359. doi 10.1029/2002JB001868

Narteau, C., Shebalin, P., and Holschneider, M., Loading rates in Valifornia inferred from aftershocks, *Nonlinear Processes Geophys.*, 2008, vol. 15, pp. 245–263.

Narteau, C., Byrdina, S., Shebalin, P., and Schorlemmer, D., Common dependence on stress for the two fundamental laws of statistical seismology, *Nature*, 2009, vol. 462, no. 3, pp. 642–646. doi 10.1038/nature08553

Nelder, J. and Mead, R., A simplex method for function minimization, *Comput. J*, 1965, vol. 7, pp. 308–312.

Nur, A. and Booker, J.R., Aftershocks caused by pore fluid flow?, *Science*, 1972, vol. 175, pp. 885–888.

Ojala, I.O., Main, I.G., and Ngwenya, B.T., Strain rate and temperature dependence of Omori law scaling constants of ae data: implications for earthquake foreshock-aftershock sequences, *Geophys. Rev. Lett.*, 2004, vol. 31, L24617. doi 10.1029/2004GL020781

Ommi, S., Zafarani, H., and Smirnov, V.B., Bayesian estimation of the modified Omori law parameters for the Iranian Plateau, *J. Seismol.*, 2016, vol. 20, pp. 953–970. doi 10.1007/s10950-016-9574-8

Ouillon, G. and Sornette, D., Magnitude-dependent Omori law: theory and empirical study, *J. Geophys. Res., Solid Earth*, 2005, vol. 110, nol .B4.

Page, R., Aftershocks and microaftershocks of the Great Alaska Earthquake of 1964, *Bull. Seismol. Soc. Am.*, 1968, vol. 58, no. 3, pp. 1131–1168.

Paterson, M.S. and Wong, T.F., *Experimental Rock Deformation—The Brittle Field*, Berlin: Springer, 2005.

Peng, Z., Vidale, J.E., and Houston, H., Anomalous early aftershock decay rate of the 2004 Mw 6.0 Parkfield, California, earthquake, *Geophys. Rev. Lett.*, 2006, vol. 33, L17307. doi 10.1029/2006GL026744

Peng, Z., Vidale, J.E., Ishii, M., and Helmstetter, A., Seismicity rate immediately before and after mainshock rupture from highfrequency waveforms in Japan, *J. Geophys. Res.*, 2007, vol. 112, B03306. doi 10.1029/2006JB004386

Pickering, G., Bull, J.M., and Sanderson, D.J., Sampling power-low distribution, *Tectonophysics*, 1995, vol. 248, pp. 1–20.

Rabinowitz, N. and Steinberg, D.M., Aftershock decay of three recent strong earthquakes in the Levant, *Bull. Seismol. Soc. Am.*, 1998, vol. 88, pp. 1580–1587.

Regel', V.R., Slutsker, A.I., and Tomashevskii, E.E., *Kineticheskaya priroda prochnosti tverdykh tel* (Kinetic Nature of the Strength of Solids), Moscow: Nauka, 1974.

Rodkin, M.V. and Tikhonov, I.N., The typical seismic behavior in the vicinity of a large earthquake, *Phys. Chem. Earth*, 2016. doi 10.1016/j.pce.2016.04.001

Rudajev, V., Vilhelm, J., and Lokajicek, T., Laboratory studies of acoustic emission prior to uniaxial compressive rock failure, *Int. J. Rock Mech. Mining Sci*, 2000, vol. 37, pp. 699−704.

Scholz, C., Experimental study of the fracturing process in brittle rock, *J. Geophys. Res.*, 1968a, vol. 73, pp. 1447−1454.

Scholz, C., Microfractures, aftershocks, and seismicity, *Bull Seismol. Soc. Am.*, 1968b, vol. 58, no. 3, pp. 1117−1130.

Schubnel, A., Thompson, B.D., Fortin, J., Gueguen, Y., and Young, R.P., Fluid-induced rupture experiment on Fontainebleau sandstone: premonitory activity, rupture propagation, and aftershocks, *Geophys. Rev. Lett.*, 2007, vol. 34, L19307. doi 10.1029/2007GL031076

Shcherbakov, R., Turcotte, D.L., and Rundle, J.E., A generalized Omori's law for earthquake aftershock decay, *Geophys. Rev. Lett.*, 2004, vol. 31, L11613. doi 10.1029/2004GL019808

Shebalin, P. and Narteau, C., Depth dependent stress revealed by aftershocks, *Nat. Commun.*, 2017, no. 8, p. 1317. doi 10.1038/s41467-017-01446-y

Shebalin, P., Narteau, C., and Holschneider, M., From alarm-based to rate-based earthquake forecast models, *Bull. Seimol. Soc. Am.*, 2012, vol. 102, no. 1, pp. 64−72.

Smirnov, V.B., Earthquake catalogs: evaluation of data completeness, *Volcanol. Seismol.*, 1998, vol. 19, pp. 497−510.

Smirnov, V.B., Prognostic anomalies of seismic regime. I. Technique for preparation of original data, *Geofiz. Issled.*, 2009, vol. 10, no. 2, pp. 7−22.

Smirnov, V.B. and Gabsatarova, I.P., Completeness of the North Caucasian earthquake catalog: calculation data and statistical estimates, *Vestn. OGGGGN RAN*, 2000, vol. 14, no. 4, pp. 35−41.

Smirnov, V.B. and Ponomarev, A.V., Seismic regime relaxation properties from in situ and laboratory data, *Izv., Phys. Solid Earth*, 2004, no. 10, pp. 807−816.

Smirnov, V.B. and Zavyalov, A.D., Seismic response to electromagnetic sounding of the Earth's lithosphere, *Izv., Phys. Solid Earth*, 2012, vol. 48, nos. 7−8, pp. 615−639.

Smirnov, V.B., Ponomarev, A.V., and Sergeeva, S.M., On the similarity and feedback in experiments on rock fracture, *Izv., Phys. Solid Earth*, 2001, no. 1, pp. 82−89.

Smirnov, V.B., Ponomarev, A.V., Benard, P., and Patonin, A.V., Regularities in transient modes in the seismic process according to the laboratory and natural modeling, *Izv., Phys. Solid Earth*, 2010, vol. 46, no. 2, pp. 104−135.

Smirnov, V.B., Ponomarev, A.V., Kartseva, T.I., Mikhailov, V.O., Chadha, R.K., and Aidarov, F., Dynamics of induced seismicity during the filling of the Nurek reservoir, *Izv., Phys. Solid Earth*, 2018, vol. 54, no. 4. doi 10.1134/S1069351318040110

Sobolev, G.A. and Ponomarev, A.V., *Fizika zemletryasenii i predvestniki* (Physics of the Earthquakes and the Precursors), Moscow: Nauka, 2003.

Stanchits, S., Vinciguerra, S., and Dresen, G., Ultrasonic velocities, acoustic emission characteristics and crack damage of basalt and granite, *Pure Appl. Geophys*, 2006, vol. 163, nos. 5−6, pp. 975−994. doi 10.1007/s00024-006-0059-5

Stanchits, S., Fortin, J., Gueguen, Y., and Dresen, G., Initiation and propagation of compaction bands in dry and wet Bentheim sandstone, *Pure Appl. Geophys.*, 2009, vol. 166, pp. 843−868. doi 10.1007/s00024-009-0478-1

Thompson, B.D., Young, R.P., and Lockner, D.A., Premonitory acoustic emissions and stick-slip in natural and smooth-faulted westerly granite, *J. Geophys. Res.*, 2009, vol. 114, B02205. doi 10.1029/2008JB005753

Utsu, T., Ogata, Y., and Matsu'ura, R.S., The centenary of the Omori formula for a decay law of aftershock activity, *J. Phys. Earth*, 1995, vol. 43, pp. 1−33.

Vilhelm, J., Rudajev, V., Ponomarev, A.V., Smirnov, V.B., and Lokajicek, T., Statistical study of acoustic emissions generated during the controlled deformation of migmatite specimens, *Int. J. Rock Mech. Mining Sci.*, 2017, vol. 100, pp. 83−89. doi 10.1016/j.ijrmms.2017.10.011

Vinogradov, S.D., On the distribution of the number of pulses by energy at rock fracture, *Izv. Akad. Nauk SSSR, Ser. Geofiz.*, 1959, no. 12, pp. 1850−1852.

Wiemer, S. and Katsumata, K., Spatial variability of seismicity parameters in aftershock zones, *J. Geophys. Res. Solid Earth*, 1999, vol. 104, no. B6, pp. 13135−13151.

Wim Dubelaar, C. and Nijland, T.G., The Bentheim sandstone: geology, petrophysics, varieties and its use as dimension stone, in *Engineering Geology For Society And Territory*, vol. 8, Lollino, G., Eds., Cham: Springer, 2015, vol. 8, pp. 557−563. doi 10.1007/978-3-319-09408-3_100

Zang, A., Wagner, F.C., and Dresen, G., Acoustic emission, microstructure, and damage model of dry and wet sandstone stressed to failure, *J. Geophys. Res.*, 1996, vol. 101, no. 8, pp. 17507−17521.

Zhurkov, S.N., Kinetic concept of the strength of solids, *Int. J. Fract. Mech.*, 1965, vol. 1, pp. 311−323.

Zhurkov, S.N., Kinetic concept of the strength of solids, *Vestn. Akad. Nauk SSSR*, 1968, no. 3, pp. 46−52.

Translated by M. Nazarenko